A Mechanistic Analysis of Sieve Tray Froth Height and Entrainment

Douglas L. Bennett
Process Engineering, Air Products and Chemicals, Inc., Allentown, PA 18195

Alan S. Kao
Environ, 4350 North Fairfax Drive, Arlington, VA 22203

Lisa W. Wong
Dept. of Chemical Engineering, 5531 Boelter Hall, University of California at Los Angeles, Los Angeles, CA 90024

A phenomenologically based model for froth height was developed using the assumption of both vapor- and liquid-continuous zones within the total froth height. The model demonstrates the importance of liquid and vapor rates and determines that the Weber number (and therefore droplet size and surface tension) has little effect on froth height.

A composite air/water database including entrainment data for both the spray and froth regimes is used to develop an entrainment correlation as a function of the ratio of tray spacing to froth height ($T_s/h_{2\phi}$) and the average froth density ($\phi_{2\phi} = h_L/h_{2\phi}$). For conditions resulting in the ratio of liquid inventory to the perforation diameter (h_L/d_H) < 4, the froth height equation requires an empirical correction for froth height, and entrainment depends on $\phi_{2\phi}$. This results from the predominantly vapor-continuous nature of the froth. For large values of h_L/d_H, the theoretical value for $h_{2\phi}$ appears adequate and entrainment is essentially independent of $\phi_{2\phi}$, since most of the liquid is contained in the liquid-continuous region located far away from the underside of the tray above. In such cases, entrainment is from a light spray on top of the liquid-continuous region, and therefore entrainment depends much less on $\phi_{2\phi}$. The different dependency of entrainment on $\phi_{2\phi}$ can be used as a method to identify the spray-froth transition. For $h_L/d_H < 2$, a spraylike condition exists; for $h_L/d_H > 2$, a frothlike condition exists.

The reported dependency of air/water system entrainment on major geometry and operating conditions is described well by the new correlation. Alternate correlations for the non-air/water entrainment data, however, are required. New methods for estimating the impact of entrainment on efficiency are given.

Introduction

The design of distillation columns requires the specification of the distance between the trays. For many processes, it is advantageous to have large numbers of distillation trays to maximize contact between the two phases and thus achieve a high degree of separation. For such applications, the accuracy of the estimate of the required tray spacing can have a significant impact on the distillation column costs. In addition, for columns that are retrayed the column height is usually fixed and the number of trays that can be included is directly related to the tray spacing. This article deals with the froth height and entrainment as they relate to operating conditions, tray design, and tray spacing.

The literature addresses the various flow regimes that can occur on a sieve tray. Although it is convenient to imagine the froth to be solely either a liquid-continuous zone with a discrete interface or a vapor-continuous region, a more accurate two-zone model will lead to a better understanding of the relationship between froth height and entrainment. The

Correspondence concerning this article should be addressed to D. L. Bennett.

froth is typically composed of a liquid-continuous region, a vapor-continuous regime where momentum and gravity forces on the liquid droplets dominate, and a mist region where drag forces on the droplet can influence the froth height. This article addresses these phenomena as they are impacted by physical properties, such as surface tension and vapor density. Since the froth structure is difficult to determine through direct measurement, measured sieve tray entrainment data in addition to the gamma ray absorption data of Hofhuis and Zuiderweg (1979) are used to judge the results of the analysis. The intent of this article is to present a phenomenologically sound approach to froth height, to derive a relationship for entrainment consistent with this mechanistic understanding, and to present a relationship that can be used to estimate the impact of entrainment on tray performance.

Background

One of the earliest works on sieve tray entrainment was that of Hunt et al. (1955). Their study found entrainment to be a function of superficial velocity and tray spacing, but independent of hole velocity. Since their investigation was based on a static system, the impact of liquid feed and outlet weir could not be determined.

Bain and Van Winkle (1961) modified the Hunt equation to include the effects of liquid feed, weir height, and hole diameter as well as plate spacing and vapor rate. Hunt's correlation requires knowledge of the froth height, which is difficult to measure due to sloshing and frothing of the liquid. Bain and Van Winkle experimentally determined the dependency of froth height on liquid rate, vapor velocity, and weir height. This correlation predicted their froth height data with an average deviation of less than 7%, while the empirical correlation they developed for entrainment represented 90% of their air/water experimental data within 25% maximum deviation. To extend the correlation to a nonair/water system, they offered without verification a correction for surface tension and density.

Fair (1961) developed a method for the prediction of sieve tray flooding, based on allowable velocities from Souders and Brown (1934). He then correlated published air/water entrainment data with approach to flooding. In order to use this method for design purposes, flooding data are required and must either be previously known or determined from similar equipment.

Kister et al. (1981) proposed that the mechanism for entrainment differed between froth (liquid-continuous) and spray (vapor-continuous) regimes. They proposed that in the froth regime, most holes are bubbling; so entrainment is primarily caused by liquid sheet breakup during and after bubble and foam generation. In this regime, increasing the liquid flow while maintaining constant vapor flow rate will increase the froth height. Therefore the emergent bubbles will break up at a level closer to the tray above, which increases entrainment. The spray regime is characterized by continuously jetting holes, which result in atomization of liquid by the vapor jets passing through the holes. In the spray regime, increasing the liquid flow rate will suppress the amount of jetting at the holes, thus decreasing entrainment. Using air/water data, the authors proposed a correlation for entrainment in the spray regime, accounting for some tray geometry effects and flow rate. Their correlation was later modified to include nonair/water systems by Kister and Haas (1988). For froth regimes in air/water systems, Kister and Haas (1988) modified Hunt's equation by combining it with Colwell's correlation (1981) for clear liquid height and including an additional term to correct for nonuniformity of the froth. Colwell's correlation for clear liquid height is a function of a Froude number that is based on the clear liquid height, thus requiring an iterative solution for this quantity.

Zuiderweg (1982) correlated previously published nonair/water data (Sakata and Yanagi, 1979) by relating the liquid and vapor properties to the average two-phase density. His analysis showed entrainment to be a strong function of the ratio of the froth height and tray spacing. The relationship between the froth height and the two-phase density allowed Zuiderweg's equation to be applied to nonair/water system.

Stichlmair (1978) proposed a relationship between entrainment and a reciprocal Froude number, which is dependent on the height of the two-phase layer. His equation is based on the calculation of the stability of the largest droplets being entrained by vapor drag. This method does not account for the physical dimensions of the tray. Puppich and Goedcke (1987) experimentally examined the effect of different tray types on entrainment. Their results were compared to predictions from Stichlmair's equations and yielded varying degrees of agreement.

Some of the cited authors have proposed physical explanations for the observed trends of entrainment. However, previous attempts have not taken these physical explanations to the point of allowing direct tests of theories against the data.

Composite Database

To understand the mechanism by which entrainment occurs, a composite database was compiled. Air/water entrainment data were obtained from the works of Friend et al. (1960), Bain and Van Winkle (1961), Lemieux and Scotti (1969), Pinczewski et al. (1975), Lockett et al. (1976), Thomas and Ogboja (1978), and Pupich and Goedcke (1987). In addition, entrainment data for the cyclohexane/*n*-heptane and isobutane/*n*-butane systems from Sakata and Yanagi (1979) and the air–oil system from Nutter (1979) were added to the database.

The database used essentially all of the data points contained in these articles. We did, however, remove 7 sets of data contained in the Friend et al. (1960) reference. The excluded data were for a very small tray spacing of 150 mm. For these conditions, they report very high entrainment rates, which requires a high liquid fraction in the froth next to the underside of the tray above. The authors did not report froth height data for these specific data. They do report, however, froth heights of 75 to 100 mm for nearly similar conditions with higher tray spacing. We believe that the high entrainment rates observed for the small tray spacings may result from a different mechanism than occurs in trays with more typical tray spacings; for example, liquid sloshing on the tray. Sloshing on a tray with low tray spacing can result in very high entrainment values. This article does not deal with this phenomenon. We have therefore excluded these 7 data sets from the database to avoid skewing the correlation for trays with typical tray spacing.

Table 1. Air/Water and Nonair/Water Data

Parameter	Min. Value (AW)	Max. Value (AW)	Min. Value (NAW)	Max. Value (NAW)
(A_H/A_T)	0.059	0.124	0.083	0.120
d_H, m	0.00159	0.0254	0.0127	0.0254
h_W, m	0.0	0.0762	0.0381	0.0635
T_S, m	0.152	0.914	0.610	0.610
ρ_L, kg/m^3	1,000	1,000	493	770
ρ_V, kg/m^3	1.224	1.224	1.13	28.0
σ, kg/s^2	0.0735	0.0735	0.005	0.024
Q_L, m^2/s/m$_{weir}$	0.00116	0.0373	0.00007	0.0278
v_S	0.45	2.31	0.071	2.41

At times it was desirable to differentiate between data taken in the froth regime and the spray regime. Although no correlation is completely acceptable, we have used the method of Pinczewski and Fell (1982). They proposed the following correlation for the froth-to-spray transition:

$$v_s\sqrt{\rho_V} = 2.75\left(Q_L\sqrt{\rho_L}\right)^n, \tag{1}$$

where Q_L is the liquid volumetric flow rate per unit weir length, v_S is the superficial velocity of the vapor, d_H is the hole diameter, A_H/A_T is the hole fraction, and $n = 0.91d_H/(A_H/A_T)$. By defining the flow parameter, Ψ,

$$\Psi = \frac{2.75\left(Q_L\sqrt{\rho_L}\right)^n}{v_S\sqrt{\rho_V}}, \tag{2}$$

they claimed that the froth regime exists where $\Psi > 1$. Although it may actually be a limitation, a further advantage of this correlation is that this method does not require estimation of the tray liquid inventory at the froth/spray transition. Reliable liquid inventory measurements were not made for the entire database. Table 1 summarizes the flow, geometry, and property ranges for air/water (AW) and non-air/water (NAW) data.

Phenomenological Model for the Froth Height

We wish to develop a clearer understanding of the phenomena that control froth heights on distillation trays. Our mechanistic model is based on an extension of the Bennett and Grimm (1991) method for calculating the height of the froth to include droplet drag, and therefore include surface tension effects. Bennett and Grimm were interested in developing a more phenomenologically correct model for froth eddy diffusivity. In their work, they attributed eddy diffusivity to the random movement of liquid droplets within the vapor-continuous portion of the froth. They defined a Peclet number using this droplet velocity, the experimental value of the eddy diffusivity, and the froth height.

As previously mentioned, the froth is characterized as consisting of a liquid-continuous region and a vapor-continuous region. In the liquid-continuous region, the vapor is distributed as bubbles throughout the liquid inventory, with droplets being ejected, as the bubbles break, into the vapor-continuous region. Bennett and Grimm's expression for froth height is developed by assuming the height of the vapor-continuous layer is equal to the maximum height that a droplet, ejected from the liquid-continuous region, will reach. The ejection velocity is calculated assuming a full exchange of momentum from the vapor traveling through the tray perforations to the upwardly flowing liquid. When calculating the froth height, Bennett and Grimm ignored the effect of vapor drag on droplet motion. This assumption simplified their analysis, since droplet diameter no longer needed to be addressed. Of concern, however, is that lower surface tension fluids such as hydrocarbons may have smaller droplets that, due to vapor drag, could significantly alter froth height.

The following analysis allows estimates of the impact of drag forces on froth height. If we can show that the impact is small for the operating regions of interest, drag can be neglected, and surface tension will not be an important physical property. If this is so, tests using air/water systems become more relevant.

The height of the liquid droplets being ejected from the liquid-continuous layer is influenced by both gravity and vapor drag on the droplet. The governing force balance is

$$M_D\frac{d}{dt}v_D = -M_Dg \pm F_D, \tag{3}$$

where M_D and v_D are the mass and velocity of a droplet and F_D is the drag force on the droplet. Expressing F_D in terms of the drag coefficient for a sphere:

$$F_D = \frac{\pi d_D^2}{4}C_D\frac{\rho_V(v_D - v_S)^2}{2}, \tag{4}$$

where d_D is the droplet diameter, ρ_V is the vapor density, and v_S is the superficial vapor velocity. Thus Eq. 3 becomes

$$\frac{d}{dt}v_D = v_D\frac{d}{dz}v_D = -g \pm \frac{3}{4}\frac{C_D\rho_V}{d_D\rho_L}(v_D - v_S)^2. \tag{5}$$

The drag will decrease the maximum droplet height if v_S is less than v_{D0}. If v_S is greater than v_{D0}, drag will increase the maximum droplet height. Therefore the positive sign in Eq. 5 is used for $v_D < v_S$ and the negative sign for $v_D > v_S$. To account for the sign of the drag contribution, Eq. 5 can be rewritten

$$\frac{d}{dt}v_D = v_D\frac{d}{dz}v_D = -g - \frac{3}{4}\frac{C_D\rho_V}{d_D\rho_L}(v_D - v_S)|v_D - v_S|. \tag{6}$$

We will assume that the diameter of the droplet can be expressed in terms of the critical Weber number for the system, We_{Cr}, which gives a relationship between the largest stable droplet diameter and the operating conditions, such as vapor hole velocity (v_H), vapor density, liquid surface tension (σ), and hole fraction (A_H/A_T):

$$We_{Cr} = \frac{\rho_V(v_H - v_S)^2d_D}{\sigma} = \frac{\rho_Vv_S^2d_D}{\sigma}\left(\frac{1}{(A_H/A_T)} - 1\right)^2. \tag{7}$$

The critical Weber number gives an indication of the largest stable droplet size under the given operating conditions and commonly ranges from 10 to 20 for low viscosity fluids (Fair et al., 1984). For our purposes, we have chosen to use an intermediate value of 15. Substituting Eq. 7 into Eq. 6 and making the equation dimensionless by normalizing with respect to the initial conditions, we can determine the dimensionless groupings on which v_D depends:

$$V\frac{dV}{d\xi} = -\frac{1}{Fr} - C_1\frac{We}{We_{Cr}}(V - V_S)|V - V_S| \tag{8}$$

where

$$V = \frac{v_D}{v_{D0}}, \quad V_S = \frac{v_S}{v_{D0}}, \quad \xi = \frac{z}{h_{Fe}}, \quad Fr = \frac{v_{D0}^2}{gh_{Fe}}, \quad C_1 = \frac{3}{4}C_D,$$

$$We = \frac{h_{Fe}\rho_V K_S^2}{\sigma}\left(\frac{1}{(A_H/A_T)} - 1\right)^2, \quad \text{and} \quad K_S^2 = v_S^2\frac{\rho_V}{\rho_L}.$$

As was done by Bennett and Grimm (1991), we will assume that the height of the liquid-continuous region is approximated by h_{Fe}, the effective froth height developed by Bennett et al. (1983). The variable v_{D0} refers to the ejection velocity of the droplets leaving the effective froth layer. This velocity was previously derived from a trajectory model (Bennett and Grimm, 1991) to be

$$v_{D0} = 3K_S\sqrt{\frac{\sqrt{3}}{(A_H/A_T)\phi_e}}, \tag{9}$$

where the effective froth density (ϕ_e), effective froth height (h_{Fe}), and weir coefficient (C) are given by Bennett et al. (1983):

$$\phi_e = \exp[-12.55K_S^{0.91}] \tag{10}$$

$$h_{Fe} = h_W + C\left(\frac{Q_L}{\phi_e}\right)^{2/3} \tag{11}$$

$$C = 0.501 + 0.439\exp[-137.8h_W]. \tag{12}$$

The drag coefficients for the liquid droplets are given by Hughes and Gilliland (1952). The effective froth density and effective froth height are related to the clear liquid height, h_L, by

$$h_L = \phi_e h_{Fe}. \tag{13}$$

The air/water and non-air/water data expressed in terms for these redefined system parameters are summarized in Table 2.

For large droplets, the contribution of the drag force is negligible compared to gravity. In this case, we will neglect drag and Eq. 8 can be integrated from the initial condition $V(\xi = 1) = 1$ to yield an expression for $V(\xi)$:

Table 2. System Parameters

Parameter	Min. Value (AW)	Max. Value (AW)	Min. Value (NAW)	Max. Value (NAW)
K_S, m/s	0.0158	0.081	0.017	0.122
ϕ_e	0.28	0.75	0.158	0.737
h_{Fe}, m	0.0169	0.145	0.052	0.162
h_L, m	0.0073	0.0481	0.017	0.064
Fr	0.134	9.29	0.084	12.3
We	0.015	1.81	0.196	1,535
V_S	1.029	1.941	0.122	1.714

$$V(\xi) = \sqrt{1 - \frac{2}{Fr}(\xi - 1)}. \tag{14}$$

The maximum height a droplet can travel defines the height of the two-phase froth, $h_{2\phi}$, which is determined by solving Eq. 14 for $V(\xi_{\max}) = 0$:

$$\xi_{\max,ND} = \frac{h_{2\phi,ND}}{h_{Fe}} = 1 + \frac{Fr}{2}. \tag{15}$$

For cases where the drag force is not negligible, Eq. 8 must be integrated to determine the froth height. This is difficult to do analytically. For such conditions, our solution for $h_{2\phi}$ is based on numerical integration of Eq. 8:

$$\xi_{\max,WD} = \frac{h_{2\phi,WD}}{h_{Fe}} = 1 + \int_0^1 \frac{V}{\frac{1}{Fr} + C_1\frac{We}{We_{cr}}(V - V_s)|V - V_s|}. \tag{16}$$

The plots in Figures 1a–1f compare the exact solution for the froth height from Eq. 16 under various ranges of operating conditions with the solution given by Eq. 15, which ignores the contribution of drag. Holding the superficial vapor velocity constant at a value greater than the droplet ejection velocity ($V_S > 1$), the vapor drag will carry liquid droplets higher than the maximum that they would reach if there was no drag contribution, thus the froth height profiles are shifted upward from the no-drag solution. The magnitude of the drag contribution is determined by the Froude and Weber numbers.

From these plots, it is apparent that drag is most significant at high superficial velocities. For the plots for $V_S = 2.0$, Figure 1a and 1b, the difference between the solutions neglecting and including drag is less than 10% only for very low Weber numbers. Since the superficial vapor velocity is twice as large as the initial droplet velocity, this small sensitivity to drag is expected.

At lower values of V_S, as shown in Figure 1c and 1d, the froth height determined from numerically integrating Eq. 16 can be predicted within 10% by using the no-drag solution given by Eq. 15 for the experimental range of Weber number and a reasonably large range of Froude number. For the case where V_S is less than unity, Figure 1e and 1f, the effect of drag is opposite of what was observed in the other two cases. Since the initial droplet velocity is greater than the superficial vapor in this case, the vapor phase will slow down the

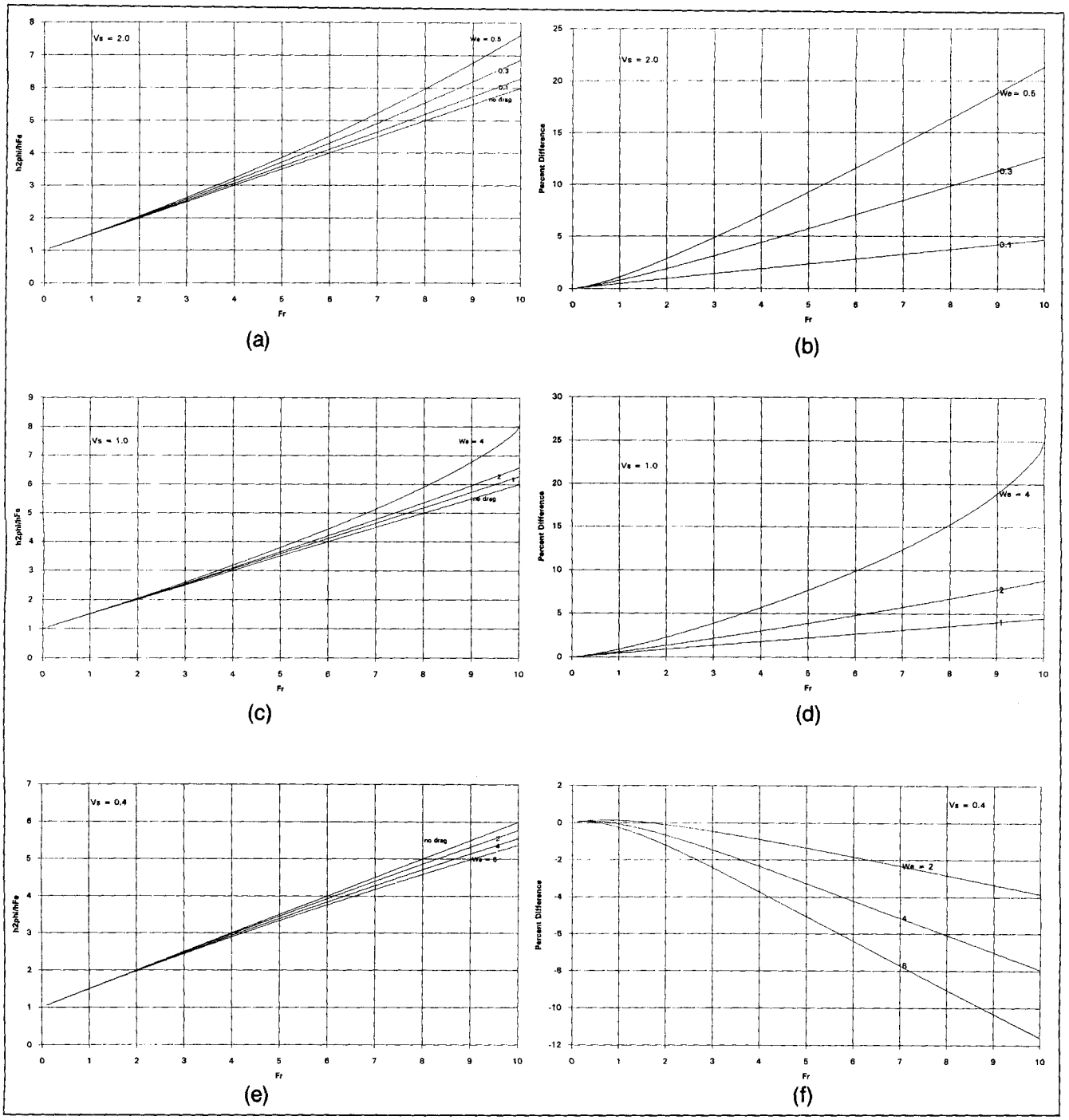

Figure 1. Effect of Froude number on froth height and percent difference between drag and no-drag solutions.

projected droplet; thus the maximum height the droplet reaches is lower than it would be without drag. However, except for the cases of extremely large Weber numbers, this effect is essentially negligible.

Although drag forces are more important for lower surface tension fluids, such as hydrocarbons, drag forces do not substantially impact froth height for most typical operating conditions. Therefore, the simpler conditions for $h_{2\phi}$ that neglect drag forces will be used as a basis for tray spacing selection.

Adjustment to the Expression for Froth Height

Although visual measurements of $h_{2\phi}$ are very difficult, we can compare Eq. 15 against the gamma scan data of Hofhuis and Zuiderweg (1979). They report the ratio of the local density within the froth to that of pure liquid. Their Figures 5–7 plot this ratio vs. position above the tray floor. Two of their data sets illustrated in their Figure 5 are for very low vapor rates, yielding values for ϕ_e greater than 0.55. The remaining data sets are in line with more normal tray operation. For the two very low vapor flow rate conditions, Eq. 15 underpre-

dicted the measured froth height by about 5 cm. For all remaining sets of data, Eq. 15 underpredicted froth height by an average of just under 3 cm. Equation 15 would be expected to underestimate the froth height if Eq. 9 underpredicts the maximum droplet ejection velocity, v_{D0}. The assumptions used to calculate v_{D0}, as reported in Bennett and Grimm (1991), require that the liquid velocity profile in the vicinity of the liquid–vapor interface is fully developed. If the velocity profile is not fully developed, Eq. 9 will underpredict the ejection velocity, v_{D0}. It is reasonable to expect that h_L/d_H is an important parameter that controls how the droplet ejection velocity approaches v_{D0}. At smaller values of h_L/d_H, the ejection velocity would be greater than v_{D0}; at larger values of h_L/d_H, the maximum ejection velocity should approach v_{D0}. The Hofhuis and Zuiderweg data show that above a value for h_L/d_H of about 6, the observed froth height is in excellent agreement with Eq. 15. The entire set of data can be correlated by

$$\frac{h_{2\phi}}{h_{Fe}} = 1 + \left(1 + 6.9\left(\frac{h_L}{d_H}\right)^{-1.85}\right)\frac{Fr}{2} \tag{17}$$

Equation 17 underestimates $h_{2\phi}$ by an average of less than 1 cm. It is interesting to note that Eq. 15 predicts that for a particular tray geometry and liquid rate, froth height is solely a function of K_S^2/gh_L. This is identical to the observations of Hofhuis and Zuiderweg. This correlation for $h_{2\phi}$ is clearly for conditions when the tray above is not interfering with the droplet trajectory.

Entrainment in the Froth Regime and Its Relationship to Tray Spacing and Operating Conditions

The previous analysis has shown that the calculated value for the froth height, $h_{2\phi}$, is relatively independent of the Weber number and primarily a function of the Froude number. This prediction can be tested against the entrainment database. In addition, our desire is to develop a correlation for entrainment.

Letting $\dot{m}_L$ and $\dot{m}_V$ represent the mass flux of entrained liquid and the mass flux of vapor approaching the tray deck and with α as the local volumetric fraction of the vapor, a mass balance gives

$$\dot{m}_L = C_f v_D (1-\alpha)\rho_L \tag{18}$$

$$\dot{m}_V = v_S \rho_V, \tag{19}$$

where $\dot{m}_L$, $\dot{m}_V$, v_D, and α are all functions of dimensionless height, ξ, and C_f is the fraction of liquid contacting the underside of the tray above that passes through the tray. The ratio of the two mass fluxes is the normalized entrainment, E:

$$E = C_f \frac{v_D}{v_S}\frac{\rho_L}{\rho_V}(1-\alpha) = C_f \frac{V}{V_S}\frac{\rho_L}{\rho_V}(1-\alpha). \tag{20}$$

Considering Eq. 20 together with Eqs. 14 and 9,

$$E\sqrt{\frac{\rho_V}{\rho_L}} = 3C_f(1-\alpha)\sqrt{\left(1-\frac{2}{Fr}(1-\xi)\right)\left(\frac{\sqrt{3}}{(A_H/A_T)\phi_e}\right)}. \tag{21}$$

The dependency of entrainment on $(\rho_L/\rho_V)^{1/2}$ is predicted, but later we compare this prediction with the entire database, which contained a variation in ρ_L/ρ_V from about 20 to nearly 1,000. This comparison shows that entrainment is dependent upon ρ_L/ρ_V.

Information about α as a function of ξ is unavailable. Our approach is to use Eq. 20 as a guide to identify correlation groupings. It is reasonable to assume that the froth density, which is defined by $\phi = 1-\alpha$, is scaled to ϕ_e, therefore:

$$\phi = 1-\alpha = \phi_e f(\xi). \tag{22}$$

Substituting Eq. 22 into Eq. 21 and using the definition of the clear liquid height (Eq. 13),

$$E\sqrt{\frac{\rho_V}{\rho_L}} = 3C_f\phi_e f(\xi)\sqrt{\left(1-\frac{2}{Fr}(1-\xi)\right)\left(\frac{\sqrt{3}}{(A_H/A_T)\phi_e}\right)}. \tag{23}$$

Evaluating this equation at the location equal to the tray spacing, T_S, the dimensionless groupings of importance for E are identified to be:

$$E\sqrt{\frac{\rho_V}{\rho_L}} = f_1\left(\frac{T_S}{h_{Fe}}, \frac{h_L}{h_{Fe}}, \frac{A_H}{A_T}, Fr, C_f\right). \tag{24}$$

We would like to reduce the number of groupings. Repasky et al. (1992) report that C_f may be a constant and we can therefore drop this term. It is possible that the dependency of E on A_H/A_T and Fr is due to the choice of h_{Fe} to normalize z. As an alternative to h_{Fe}, the froth height $h_{2\phi}$ is substituted. Since $h_{2\phi}$ is dependent upon A_H/A_T and Fr, this could reduce the correlation dependency on these groupings. Therefore, the following groupings may be adequate:

$$E\sqrt{\frac{\rho_V}{\rho_L}} = f_2\left(\frac{T_S}{h_{2\phi}}, \phi_{2\phi}\right), \tag{25}$$

where $\phi_{2\phi} \equiv h_L/h_{2\phi}$. The data will show whether these assumptions are valid. Much of the entrainment data is for conditions when the tray spacing is less than the calculated froth height ($T_S/h_{2\phi} < 1$). Operating a tray under such conditions is clearly possible and, in fact, common in some types of applications. Regardless of the value of $T_S/h_{2\phi}$, an equation for $h_{2\phi}$ will be used that ignores the presence of the tray above. If successful, this assumption vastly simplifies the correlation.

Analysis of the Air/Water Database

The air/water database is substantially broader than the non-air/water database and includes data from a wide range

of tray geometry and operating conditions. The functional relationship between entrainment and the two dimensionless groupings can be determined for the air/water data alone. Using the Pinczewski and Fell (1982) criteria for the froth/spray transition, the air/water froth data yield the following correlation for entrainment:

$$E_{\text{froth}} = 0.00405\phi_{2\phi}^{0.00095}\left(\frac{T_S}{h_{2\phi}}\right)^{-1.967}\left(\frac{\rho_L}{\rho_V}\right)^{0.5}, \quad (26)$$

where $h_{2\phi}$ is calculated from Eq. 15. The power for the first grouping is essentially zero. There was no variation in the density ratio for the air/water data; ρ_L/ρ_V was always equal to 817. However, the variation in $\phi_{2\phi}$ was from 0.01 to 0.70. It appears that the air/water entrainment data are reasonably correlated by $T_S/h_{2\phi}$ alone. Therefore, for the froth regime and ambient conditions for air/water,

$$E_{\text{froth}} = 0.125\left(\frac{T_S}{h_{2\phi}}\right)^{-1.95} \quad (27)$$

with $h_{2\phi}$ again being calculated from Eq. 15.

As mentioned earlier, the froth height data of Hofhuis and Zuiderweg (1979) is more accurately correlated by Eq. 17 than by Eq. 15. Equation 17 can also be used to develop a correlation for entrainment. Again, the power for the first grouping in Eq. 26 is found to be approximately zero. Using Eq. 17, the correlation for entrainment for the froth regime and ambient conditions for air/water is

$$E_{\text{froth}} = 0.0469\left(\frac{T_S}{h_{2\phi}}\right)^{-1.86}. \quad (28)$$

For other values of ρ_L/ρ_V, the air/water-based froth flow correlation becomes

$$E_{\text{froth}} = 0.00164\left(\frac{T_S}{h_{2\phi}}\right)^{-1.86}\left(\frac{\rho_L}{\rho_V}\right)^{0.5}. \quad (29)$$

Comparison of Air/Water Froth Regime Entrainment Correlation against Observed Trends

Equation 29 can be expanded by using Eq. 17 for $h_{2\phi}$ and the expression for Fr:

$$E_{\text{froth}} = 0.00164\left(\frac{K_S^2}{g\phi_e T_S}\right)^{1.86} \times\left(\frac{gh_L}{K_S^2} + \frac{9\sqrt{3}}{2}\frac{1}{(A_H/A_T)}\left[1+6.9\left(\frac{d_H}{h_L}\right)^{1.85}\right]\right)^{1.86}\left(\frac{\rho_L}{\rho_V}\right)^{0.5}. \quad (30)$$

This expression is useful in identifying trends and comparing these to the observations in Kister et al. (1981) and Kister and Haas (1988). Equation 30 provides insight and support to their observations. In addition, an expression for conditions yielding a minimum in entrainment as a function of liquid rate will be derived from Eq. 30. Kister and Haas (1988) and others have proposed this as an indication of the jetting to froth transition.

Equation 30 shows that the important parameters are the Froude-type numbers $K_S^2/\phi_e g T_S$ and K_S^2/gh_L and the geometry parameters d_H/h_L and A_H/A_T.

Effect of hole diameter

Kister and Haas (1988) report that at high vapor rates, low liquid rates, and large hole diameters, entrainment rises significantly with d_H. At small values of d_H and higher values of liquid rate, d_H has little significance. Equation 30 is consistent with these observations. At low liquid rates and high vapor rates, the groupings containing d_H/h_L become important, resulting in a significant dependency on d_H. At small values of d_H and higher values of K_S^2/gh_L, the importance of d_H/h_L becomes small.

Effect of tray spacing

Kister and Haas found that entrainment is inversely proportional to tray spacing raised to a power of 2 to 3. Equation 30 suggests that the power is closer to 2.

Effect of fractional hole area

Kister and Haas report that at high vapor velocities, low liquid flow rates, and low values of A_H/A_T, entrainment rises rapidly with decreasing A_H/A_T. At low vapor rates, high liquid rates, and high values of A_H/A_T, entrainment is only slightly dependent on hole area. Equation 30 shows that for high values of K_S^2/gh_L, specifically high vapor velocities and low liquid flow rates, entrainment increases rapidly as A_H/A_T decreases. However, at low values of vapor rate and high values of liquid rate, A_H/A_T is less important, especially when A_H/A_T is large.

Effect of outlet weir height

Kister and Haas report a complex dependency between entrainment and outlet weir height. For low weirs and low liquid rates, entrainment is reported to decrease. They also report an increase in entrainment with outlet weir when liquid rate is high and vapor is low. Finally, they report that conditions with high weirs with high vapor and liquid flow rates give little dependency of entrainment on weir height. Equation 30 states that the outlet weir height is only important through its impact on h_L. These results are consistent with the preceding observations, but will be discussed later.

Effect of vapor velocity

Kister and Haas report that at high vapor rates and low liquid rates, entrainment is proportional to the vapor velocity raised to a power of 4 to 5. At other conditions, entrainment is proportional to the vapor velocity raised to a power of 2 to 3. According to Eq. 30, the dependency of entrainment on vapor rate (K_S) depends upon the importance of gh_L/K_S^2. For low liquid rates and high vapor rates, gh_L/K_S^2 is less

important and entrainment depends on K_S raised to a power of about 5. As gh_L/K_S^2 becomes larger, the dependency on K_S becomes less. At a typical value for gh_L/K_S^2 of about 100, the entrainment depends upon K_S raised to the power 3.

Effect of liquid inventory and liquid flow rate

Kister et al. (1981) and others have reported that as liquid rate increases, entrainment can go through a minimum. Porter and Jenkins (1979) proposed that this minimum coincides with the spray to mixed froth/spray transition. Kister et al. (1981) proposed that the minimum corresponds to a transition at the orifice from bubbling to intermediate jetting. As reported by Kister et al., the correlation proposed by Porter and Jenkins to predict this minimum is not particularly successful.

Equation 30 can be used to predict this minimum. Differentiating with respect to h_L/d_H and setting the derivative equal to zero, the value of h_L/d_H corresponding to the minimum is

$$\left(\frac{h_L}{d_H}\right)_{\min} = 5\left(\frac{K_S^2}{gd_H(A_H/A_T)}\right)^{0.35}. \tag{31}$$

The functionality of Eq. 31 is similar to the Hofhuis and Zuiderweg (1979) correlation for the froth/spray transition:

$$\left(\frac{h_L}{d_H}\right)_{\text{transition}} = \frac{1.07}{(A_H/A_T)^{1/3}}\left(\frac{K_S^2}{gd_H(A_H/A_T)}\right)^{1/3}. \tag{32}$$

It is interesting to note that the presence of a minimum does not require a flow regime transition, but only requires the recognition that the exchange of momentum between vapor and liquid is incomplete and that h_L/d_H is an important parameter in controlling this exchange of momentum. It is also interesting to observe that this minimum is near the conditions when the flow regime is variant.

Air/Water Entrainment in the Spray Regime and its Relationship to Tray Spacing and Operating Conditions

Equations 18 through 25 should be equally valid whether the tray is operating in the froth or spray regime. Repeating Eq. 25,

$$E\sqrt{\frac{\rho_V}{\rho_L}} = f_2\left(\frac{T_S}{h_{2\phi}}, \phi_{2\phi}\right). \tag{25}$$

As shown in Eq. 26, the froth flow air/water data indicated no dependency upon $\phi_{2\phi}$. We believe that this is due to the major portion of the liquid being contained in the liquid-continuous region, bounded by the tray deck and h_{Fe}. The entrainment rate must be dependent upon the local froth density near the tray above. For froth-type flows, this local froth density is apparently relatively independent of the average froth density, $\phi_{2\phi}$.

For the spray regime, much of the liquid is in the vapor-continuous regime. We would expect, therefore, a greater dependency of entrainment on $\phi_{2\phi}$. Borrowing from the analysis of the froth flow data, we assumed for the spray regime a correlation format of

$$E_{\text{spray}}\sqrt{\frac{\rho_V}{\rho_L}} = a\left(\frac{T_S}{h_{2\phi}}\right)^b f(\phi_{2\phi}) \tag{33}$$

where a and b are constants which will be determined later, and

$$f(\phi_{2\phi}) = \phi_{2\phi}^{\beta}. \tag{34}$$

We would expect that β approaches zero for the froth regime and approaches unity for the spray regime. A hyperbolic tangent function has the expected bounds. Data regression will show that the following is reasonable:

$$\beta = 0.5\left(1 - \tanh\left[1.3\ln\left(\frac{h_L}{d_H}\right) - 0.15\right]\right). \tag{35}$$

We will also assume a relationship for $h_{2\phi}$ that is similar to Eq. 17,

$$\frac{h_{2\phi}}{h_{Fe}} = 1 + \left(1 + c\left(\frac{h_L}{d_H}\right)^d\right)\frac{Fr}{2}. \tag{36}$$

where c and d are constants.We again used the Pinczewski and Fell (1982) method to identify the spray data within the composite air/water database. Using these spray data, we derived the following constants for the spray regime:

$$E_{\text{spray}} = 0.0050\left(\frac{T_S}{h_{2\phi}}\right)^{-1.26} f(\phi_{2\phi})\left(\frac{\rho_L}{\rho_V}\right)^{0.5} \tag{37}$$

where

$$\frac{h_{2\phi}}{h_{Fe}} = 1 + \left(1 + 4.77\left(\frac{h_L}{d_H}\right)^{-3.29}\right)\frac{Fr}{2} \tag{38}$$

and $f(\phi_{2\phi})$ is given by Eq. 34 and Eq. 35.

Comparison of Air/Water Spray and Froth Regime Entrainment Correlations

Using the expressions for $h_{2\phi}$ and Fr, Eq. 37 can be expanded to a form similar to Eq. 30:

$$E_{\text{spray}} = 0.0050\left(\frac{K_S^2}{g\phi_e T_S}\right)^{1.26} \times \left(\frac{gh_L}{K_S^2} + \frac{9\sqrt{3}}{2}\frac{1}{(A_H/A_T)}\left[1 + 4.77\left(\frac{d_H}{h_L}\right)^{3.29}\right]\right)^{1.26} \times f(\phi_{2\phi})\left(\frac{\rho_L}{\rho_V}\right)^{0.5} \tag{39a}$$

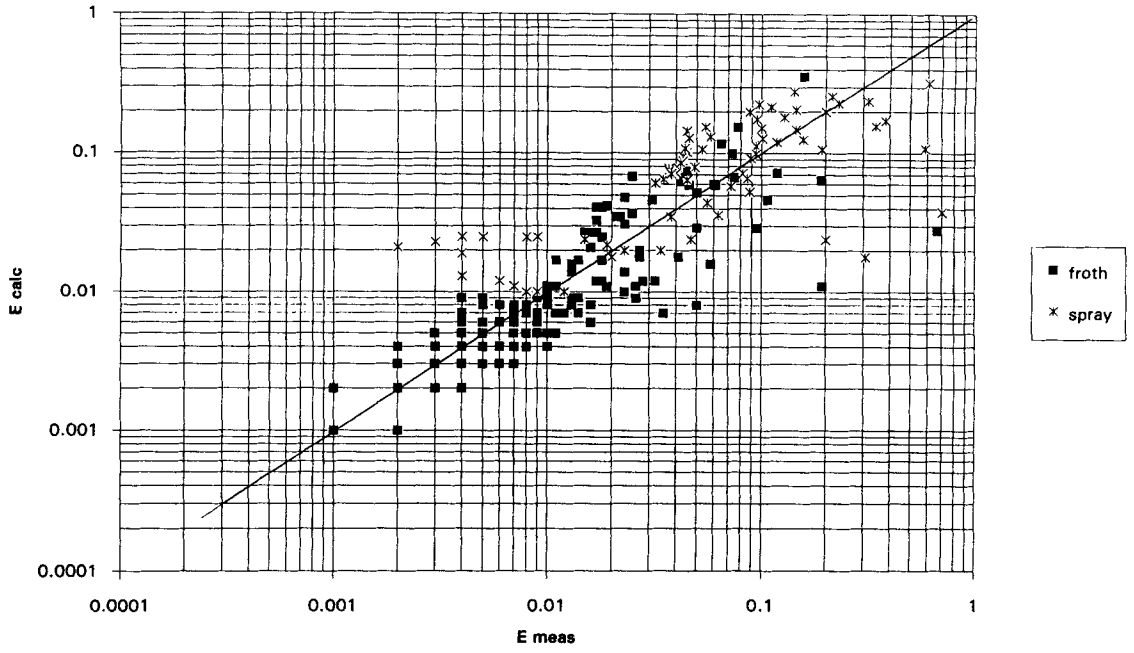

Figure 2. Parity plot using separate spray and froth regime correlations.
Spray and froth regime data separated using Pinczewski and Fell (1982).

If we reduce Eq. 39a to those conditions where we are clearly in the spray regime, for example, h_L/d_H less than about 0.5, Eq. 39a can be simplified to

$$E_{\text{spray}} = 0.476\left(\frac{\rho_L}{\rho_V}\right)^{0.5}\phi_{2\phi}\left(\frac{d_H}{h_L}\right)^{4.14}\left(\frac{K_S^2}{g\phi_e T_S(A_H/A_T)}\right)^{1.26}. \tag{39b}$$

Equation 39b can be used to contrast air/water entrainment in the spray regime to that in the froth regime.

Effect of the average froth density

The most significant difference between entrainment in the froth and in the spray regimes is the dependency of entrainment on the average froth density, $\phi_{2\phi} = h_L/h_{2\phi}$. In the spray regime, entrainment is approximately proportional to $\phi_{2\phi}$. In the froth regime, entrainment has little dependency on $\phi_{2\phi}$.

Effect of hole diameter

In the spray regime, entrainment is very strongly dependent upon the perforation diameter. In the froth regime, especially when h_L/d_H is greater than about 10, entrainment is independent of d_H.

Effect of vapor rate

In the froth regime, we found from Eq. 30 that entrainment varied with vapor rate raised to a power of about 3. For typical conditions in the spray regime, at a constant liquid rate, h_L varies with K_S to about the $-1/3$ power and ϕ_2 is approximately inversely proportional to K_S. Equation 39b shows, therefore, that for the spray regime and at constant liquid rate and $\phi_{2\phi}$, entrainment varies with K_S to a power of about 5 or 6.

Effect of tray spacing

In the froth regime, we found that entrainment was inversely proportional to the tray spacing raised to a power of 2 to 3. In the spray regime, entrainment appears to be less dependent upon the tray spacing. This probably results from the greater uniformity of the froth density that occurs in the spray regime.

Overall Air/Water Correlation for Entrainment—Comments on Froth/Spray Transition

Figure 2 is a parity plot for the entire database, using as appropriate Eq. 29 (or 30) for the froth regime data and Eq. 37 (or 39a) for the spray regime data. We have again used the Pinczewski and Fell (1982) correlation to separate the spray and froth regime databases. It is appropriate, however, to question the need for such a criterion. Equations 30 and 39a show that there are significant similarities in the respective spray and froth relationships between entrainment and operating conditions. We believe that the most important distinguishing characteristic is the dependency of entrainment on the average froth density. Equations 34 and 35 give a reasonable method of describing this relationship. The parameter h_L/d_H is of significance. As h_L/d_H exceeds about 2, β approaches zero and entrainment is no longer a function of $\phi_{2\phi}$. As h_L/d_H is less than about unity, β approaches unity, and entrainment is proportional to $\phi_{2\phi}$. We propose that the reasonable and simple hydrodynamic criterion for the froth/spray transition is

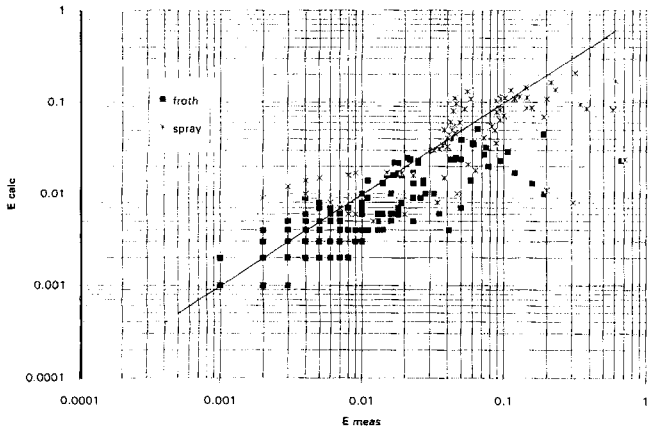

(a)

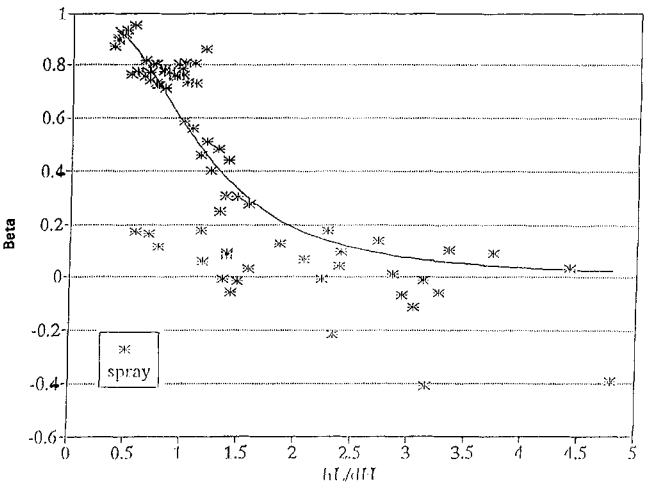

(b)

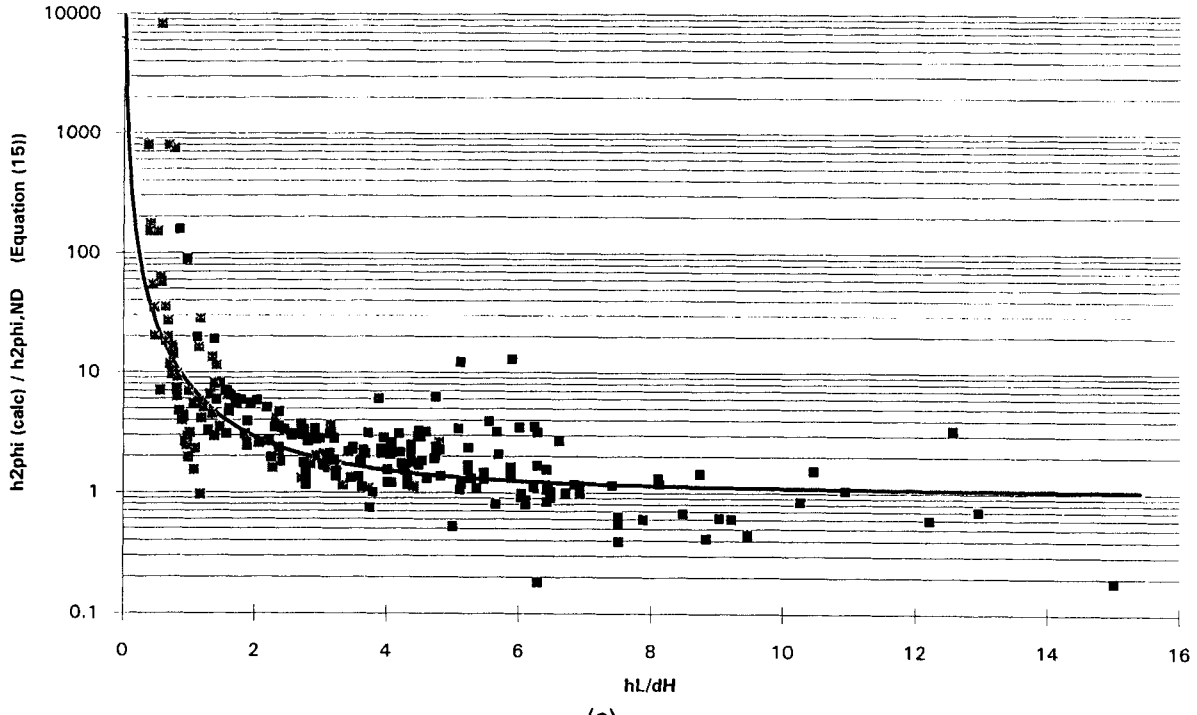

(c)

Figure 3. (a) Parity of air/water entrainment using overall correlation; (b) β as a function of h_L/d_H; (c) back-calculated froth height vs. h_L/d_H.

$$\frac{h_L}{d_H} < 1 \qquad \text{Spraylike regime} \qquad (40a)$$

$$1 < \frac{h_L}{d_H} < 2 \qquad \text{Transitional} \qquad (40b)$$

$$\frac{h_L}{d_H} > 2 \qquad \text{Frothlike regime} \qquad (40c)$$

The composite database can be used to generate an overall correlation for entrainment. A correlation of the form of Eq. 25 will be assumed. Since h_L/d_H seems to be a primary parameter, we will use the following format for the correlation:

$$E\sqrt{\frac{\rho_V}{\rho_L}} = a\left(\frac{T_S}{h_{2\phi}}\right)^{b+c(h_L/d_H)^d} \phi_{2\phi}^{\beta}, \qquad (41)$$

where β is defined by Eq. 35 and

$$\frac{h_{2\phi}}{h_{Fe}} = 1 + \left(1 + e\left(\frac{h_L}{d_H}\right)^f\right)\frac{Fr}{2} \qquad (42)$$

where a, b, c, d, e, and f are constants to be determined.

The composite database gives

$$E\sqrt{\frac{\rho_V}{\rho_L}} = 0.00164\left(\frac{T_S}{h_{2\phi}}\right)^{-1.86+0.26(h_L/d_H)^{-0.7}} \phi_{2\phi}^{\beta} \quad (43)$$

and

$$\frac{h_{2\phi}}{h_{Fe}} = 1 + \left(1 + 6.0\left(\frac{h_L}{d_H}\right)^{-2.5}\right)\frac{Fr}{2}. \quad (44)$$

Figure 3a shows a parity plot, using Eq. 43 to predict entrainment, for the entire composite database. Figure 3b shows the calculated value of β as a function of h_L/d_H. Since the froth data generally have values for h_L/d_H greater than 2, we have only shown the spray regime data. Figure 3c shows the back calculated froth height vs. h_L/d_H, assuming Eq. 43 is valid to calculate $h_{2\phi}$. As expected, the back-calculated froth height agrees well with the theoretical values for large values of h_L/d_H. For smaller values of h_L/d_H, the data agree reasonably well with the observed froth heights reported by Hofhuis and Zuiderweg.

Entrainment for the Nonair/Water Systems

The database also includes entrainment data for cyclohexane/*n*-heptane systems at 5 and 24 psia (34 and 165 kPa), isobutane/*n*-butane, and air/Isopar-M oil. The functionality suggested in Eq. 41 can be compared against these nonair/water data. Figure 4 is a plot of the density-corrected entrainment for the 24-psia cyclohexane/*n*-heptane database vs. $h_{2\phi\ \mathrm{calc}}/T_S$ using Eq. 44 to predict $h_{2\phi\ \mathrm{calc}}$. Each symbol corresponds to a constant liquid rate. Consistent with Eq. 43, Figure 5 is a plot of all nonair/water data and plots P vs. h_L/d_H, where P denotes the power on $T_S/h_{2\phi\ \mathrm{calc}}$. We find that at lower values of $h_L/d_H$and higher values of h_L/d_H, consistent, but different, values for P occur. A transition for all subsets occurs between a value for h_L/d_H of 1.5 to 3. This reinforces our air/water conclusion that a transition from spraylike to frothlike behavior occurs within this relatively narrow range of h_L/d_H.

A possible explanation for the different values of P can be seen if we examine the basic entrainment mass balance equations (Eqs. 18, 19 and 20). The mass balance shows that the normalized entrainment, E, is proportional to the volume fraction of liquid, $1-\alpha$, at the location of the upper tray. Figure 6 illustrates typical liquid volume fractions as a function of the vertical height above the tray deck. Although there will be some interference resulting from the placement of the tray above into the froth or spray, we would expect that the general nature illustrated in Figure 6 will still be valid when the tray above starts to penetrate the outer regions of the froth or spray. The value of P would therefore be expected to be dependent upon the variation of the volume fraction of liquid $(1-\alpha)$ with distance from the tray (z). Specifically, P should be proportional to $\partial(1-\alpha)/\partial z$, the partial derivative of the liquid volumetric fraction with respect to distance from the tray deck. Figure 6 shows that $\partial(1-\alpha)/\partial z$ (and therefore P) is larger for froth flow than for spray flow. Figure 6 also illustrates that the value for P is not necessarily constant as the distance from the tray floor changes. We believe that the different values for P seen in Figure 5 as we go from spray to froth and the different values of P for different systems results from the complex behavior of $\partial(1-\alpha)/\partial z$ within the frothlike and spraylike regimes.

The nonair/water database was divided into a spray database and a froth database using the observed change in the value of P as the selection criterion. To test the air/water entrainment correlation against the nonair/water results, we avoided the need to estimate $h_{2\phi}$ by using Eq. 30 for the froth regime and Eq. 39a for the spray regime.

The direct comparison of Eq. 30 against the nonair/water froth regime data shows that the air/water-based correlation

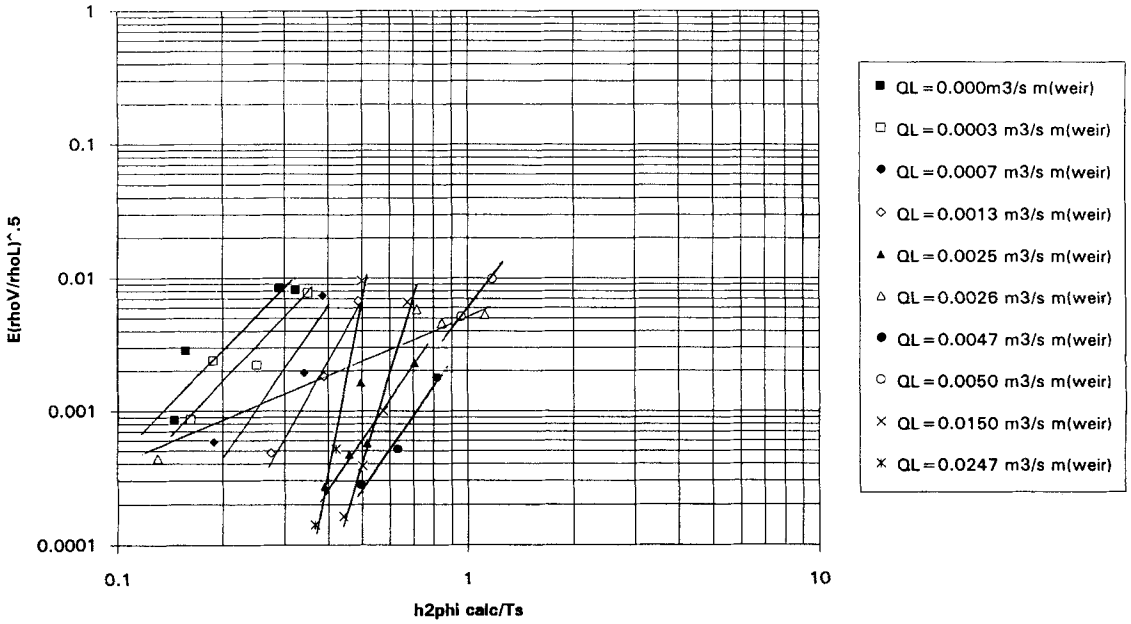

Figure 4. Density corrected entrainment vs. $h_{2f\ \mathrm{calc}}/T_S$ using Eq. 44 to predict $h_{2f\ \mathrm{calc}}$: cyclohexane/*n*-heptane, 24 psia (165 kPa).

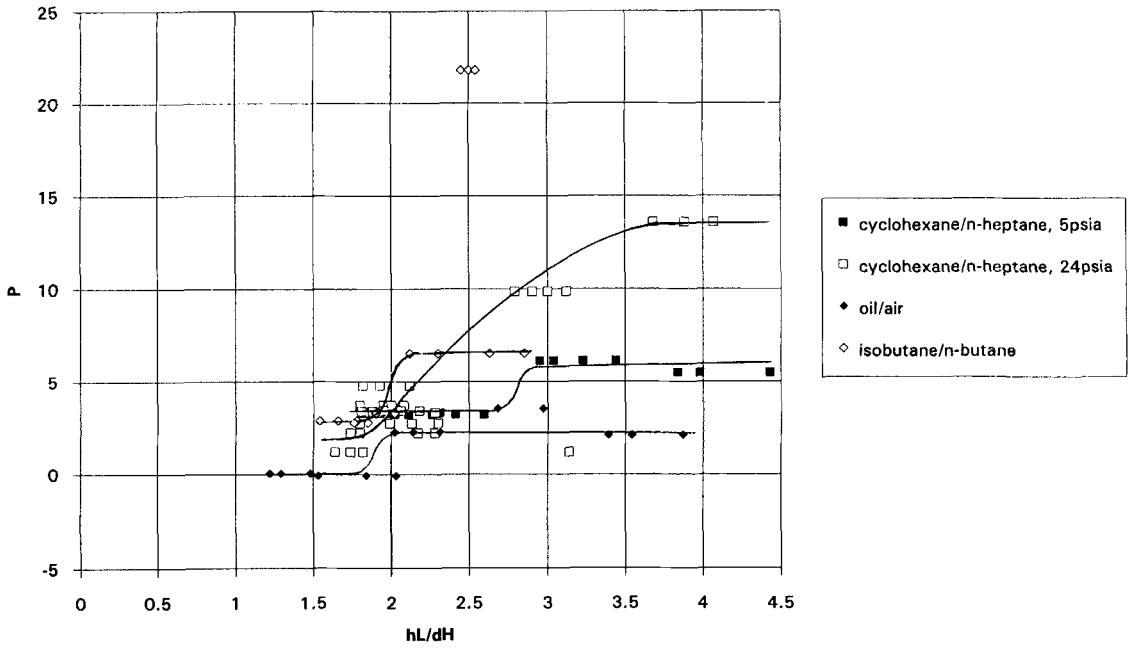

Figure 5. P vs. h_L/d_H for all nonair/water data.

overestimates entrainment for low values of observed entrainment and underestimated entrainment for higher observed values. Somewhat better agreement for the nonair/water systems was obtained using

$$E_{\text{froth}} = 0.742\left(\frac{K_S^2}{g\phi_e T_S}\right)^{2.77}\left(\frac{gh_L}{K_S^2}\right)^{1.81}\left(\frac{\rho_L}{\rho_V}\right)^{1.19}. \quad (45)$$

For the spray data, we compared the nonair/water database against the air/water spray correlation, Eq. 39a. As we saw with the froth data, the air/water-based correlation overpredicts the observed nonair/water entrainment data at low values of observed entrainment ($E < 0.01$) and underpredicts entrainment at higher values of observed entrainment. Much better agreement (within a factor of 2) was obtained throughout the range of entrainment ($0.001 \le E \le 0.4$) with

$$E_{\text{spray}} = 8\times 10^{-18}\left(\frac{K_S^2}{g\phi_e T_S}\right)^{1.56} \times\left(\frac{gh_L}{K_S^2}+2.48\frac{1}{(A_H/A_T)}\left[1+8.27\left(\frac{d_H}{h_L}\right)^{-.614}\right]\right)^{7.40} \times \phi_{\mathcal{L}\phi}^{\beta}\left(\frac{\rho_L}{\rho_V}\right)^{1.08}. \quad (46)$$

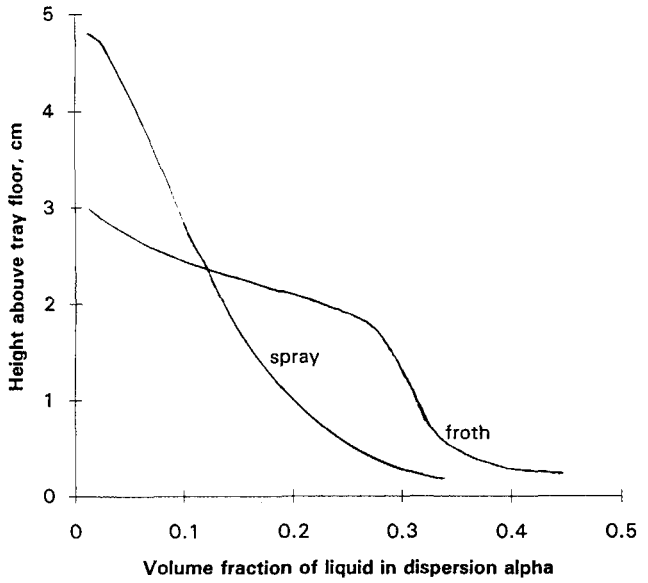

Figure 6. Typical volume fraction profiles for froth and spray as a function of z.

A parity plot for Eqs. 45 and 46 is given in Figure 7. Five points were not included in Figure 7 because they used unrealistically low liquid flow rates that were not representative of actual system conditions. We believe that the large scatter for the froth data is attributable to the observed variation in the power, P, as shown in Figure 5. This variation in P is much greater for the nonair/water frothlike data than was observed for the nonair/water spraylike data. The functionality assumed in Eq. 45 does not fully account for this variation in P. Attempts using the more general functionality, Eq. 24, were no more successful. The problem may be that Eq. 22 is an oversimplification. As we discussed, P is dependent upon $\partial(1-\alpha)/\partial z$. More froth density profile data for a variety of flow conditions and systems would be very helpful in developing a better understanding of the variation in P for various systems.

We can also compare the entire nonair/water database (spray and froth) against the overall correlation, Eqs. 42 and

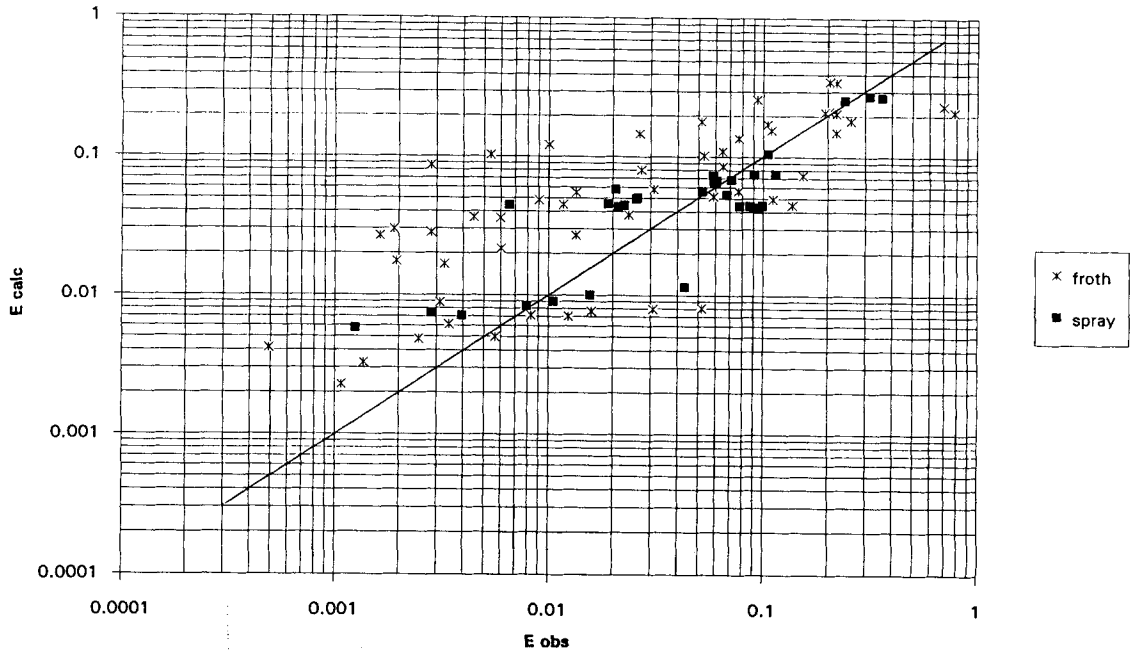

Figure 7. Parity plot of nonair/water entrainment using Eqs. 45 and 46.

43. Once again, the air/water correlation underpredicts entrainment. A correlation that is within a factor of 2 when the observed entrainment is greater than about 0.100, but overpredicts entrainment at lower values of observed entrainment is given by Eq. 47:

$$E = 0.04\left(\frac{T_S}{h_{2\phi}}\right)^{-1.04} \phi_{2\phi}^{\beta}\left(\frac{\rho_L}{\rho_V}\right)^{0.5}. \tag{47}$$

Impact of Entrainment on Tray Performance

As entrainment increases, tray performance decreases. The impact of entrainment on column performance has been calculated numerically by Lockett et al. (1983). Tables of these results are presented in Appendix B of Lockett (1986) for parallel and cross-flow tray configurations. These tables summarize the impact of a uniform entrainment flux on the Murphree tray efficiency as a function of the tray configuration, the point efficiency (E_{OG}), the stripping factor (λ_0), and the liquid Peclet number (Pe). The stripping factor is defined as:

$$\lambda_0 = \frac{mV_0}{L_0}, \tag{48}$$

where m is the slope of the equilibrium line, V_0 is the vapor molar flow rate, and L_0 is the liquid molar flow rate in the absence of entrainment. For values of E ranging from 0.1 to 0.3 kg liquid/kg vapor, λ_0 from 0.5 to 3.0, Pe from 0 to 1,000, and E_{OG} from 0.4 to 1.0, the following equation is a reasonable approximation of the published tables:

$$\frac{E_{MV}(E)}{E_{MV}(E=0)} = 1 - 0.8E_{OG}\lambda_0^{0.543}E\frac{V_0}{L_0}. \tag{49}$$

Parity plots demonstrating the agreement between the tabulated values and Eq. 49 are shown in Figure 8 for both tray configurations. This equation allows one to calculate the decrease in performance due to entrainment.

Summary and Conclusions

In this article, we have presented a phenomenologically based analysis of sieve tray entrainment in the froth and spray regimes. Based on a mechanistic analysis of the froth, in which droplets are ejected from a liquid-continuous region, a trajectory model for the droplets was developed. The maximum distance reached by the droplets defines the height of the two-phase region. The exact solution to this model was compared to an approximate solution that ignores the contribution of drag. If the drag force on the droplets from the vapor stream is significant compared to the other forces, the froth height will be different and Figure 1 is needed.

For air/water systems, the effect of drag is generally not significant and can therefore be ignored. This also applies to much but not all of the nonair/water data that were collected from the literature. The smaller droplets that result from using lower surface tension fluids are more sensitive to drag than the droplets in the air/water system. However, since these nonair/water systems also generally operate with vapor velocity ranges of $V_S < 1$, the consideration of drag will actually decrease the entrainment expected when drag is negligible.

We have also developed a correlation for entrainment based solely on the ratio of froth height to tray spacing, $h_{2\phi}/T_S$, and the average froth density $f_{2\phi} \equiv h_L/h_{2\phi}$, and the other nondimensional groupings. We developed an entrainment and froth height correlation for the larger composite air/water database. This air/water correlation consistently generates the complex reported trends between entrainment flow rates and geometry parameters.

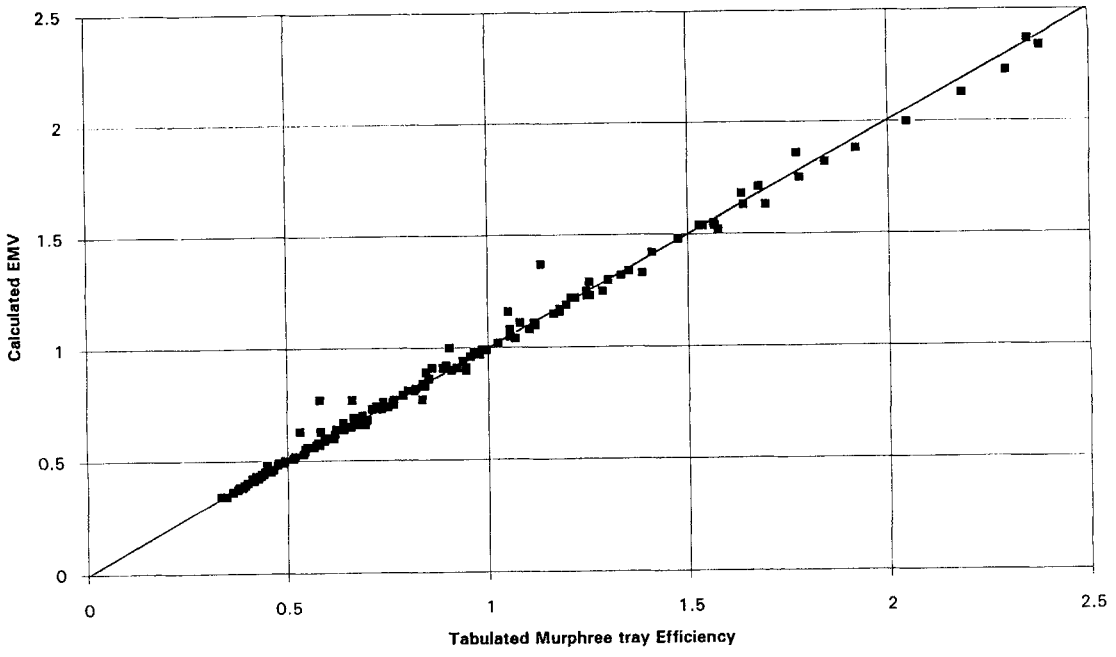

(a)

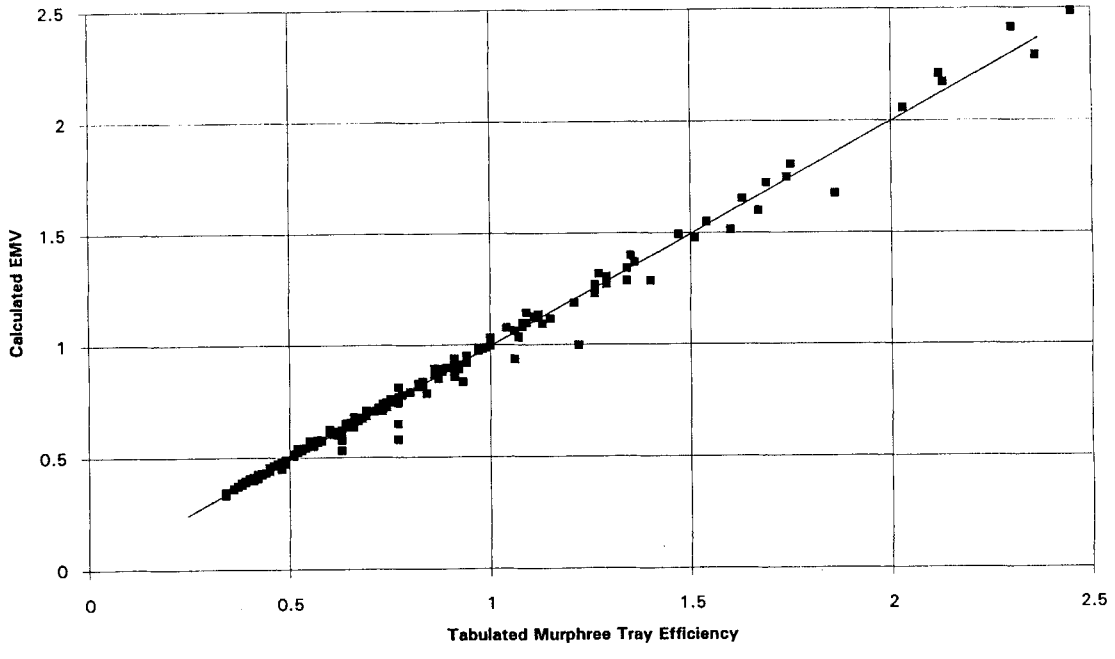

(b)

Figure 8. Effect of entrainment on Murphree tray efficiency.

(a) Parallel configuration. (b) Cross-flow configuration.

Next, we compared these air/water correlations against the less populous nonair/water database. The air/water correlations overpredicted entrainment for lower observed values and underpredicted entrainment at higher observed values. Alternative expressions are given.

The following conclusions can be made for both air/water and the evaluated nonair/water systems:

1. At h_L/d_H values less than about 2, the behavior of the vapor and liquid on a distillation tray behaves in a spraylike manner, characterized by a stronger dependency of entrainment on the average froth density, $\phi_{2\phi}$, and a less significant dependency on $T_S/h_{2\phi}$ than occurs for frothlike flow.

2. At h_L/d_H values greater than about 2, the behavior of the vapor and liquid behaves in a frothlike manner characterized by the entrainment being relatively independent of $\phi_{2\phi}$ and more significantly dependent upon $T_S/h_{2\phi}$ than seen for spraylike conditions.

3. If the spraylike/frothlike distinction is necessary, h_L/d_H

< 2 for identifying the spraylike regime and $h_L/d_H > 2$ for identifying the frothlike region is recommended.

4. Our phenomenological analysis of the froth flow mechanism predicts that the use of a density corrected entrainment, $E\sqrt{\rho_V/\rho_L}$, removes the need for additional ρ_L/ρ_V corrections. The nonair/water froth data supports that entrainment does depend upon the ratio ρ_L/ρ_V. Within the accuracy of the correlation, the predicted dependency may be correct. A small improvement is obtained for the nonair/water data by allowing this dependency to float, giving E as being about directly proportional to ρ_L/ρ_V.

5. For the air/water system Eq. 29 or Eq. 30 is our best entrainment correlation for the froth regime and Eqs. 37 and 38 or Eq. 39a is our best entrainment correlation for the spray regime. A reasonable correlation for both the spray and the froth regimes is Eqs. 43 and 44:

$$E\sqrt{\frac{\rho_V}{\rho_L}} = 0.00164\left(\frac{T_S}{h_{Fe}}\right)^{-1.86+0.26(h_L/d_H)^{-0.7}}\phi_{2\phi}^{\beta} \tag{43}$$

$$\frac{h_{2\phi}}{h_{Fe}} = 1+\left(1+6.0\left(\frac{h_L}{d_H}\right)^{-2.5}\right)\frac{Fr}{2} \tag{44}$$

where

$$\beta = 0.5\left(1-\tanh\left[1.3\ln\left(\frac{h_L}{d_H}\right)-0.15\right]\right). \tag{35}$$

6. The air/water-based correlations are not generally appropriate for nonair/water systems. Based on the data analyzed for this study, a reasonable estimate of the entrainment for froth flow is obtained from Eq. 45

$$E_{\text{froth}} = 0.742\left(\frac{K_S^2}{g\phi_e T_X}\right)^{2.77}\left(\frac{gh_L}{K_S^w}\right)^{1.81}\left(\frac{\rho_L}{\rho_V}\right)^{1.19} \tag{45}$$

and a reasonable estimate of entrainment for spray flow is given by

$$E_{\text{spray}} = 8\times10^{-18}\left(\frac{K_S^2}{g\phi_e T_S}\right)^{1.56}\left(\frac{gh_L}{K_S^2}+2.48\frac{1}{(A_H/A_T)}\right.$$
$$\left.\times\left[1+8.27\left(\frac{d_H}{h_L}\right)^{-.614}\right]\right)^{7.40}\phi_{2\phi}^{\beta}\left(\frac{\rho_L}{\rho_V}\right)^{1.08}. \tag{46}$$

An overall correlation for either the spray or froth regime that, based on our reported data, predicts within a factor of about 2 for higher values of reported entrainment is Eq. 47

$$E = 0.04\left(\frac{T_S}{h_{2\phi}}\right)^{-1.04}\phi_{2\phi}^{\beta}\left(\frac{\rho_L}{\rho_V}\right)^{0.5}, \tag{47}$$

where $h_{2\phi}$ is predicted from Eq. 44, and β is calculated from Eq. 35.

7. Froth height observations are notoriously difficult to make due to the lack of a distinct interface and its transient nature. This is especially true for the spraylike regime. Equation 44 was derived from entrainment data, and should not be regarded as a correlation for the observed froth height. The limited gamma ray observation data discussed in this article suggests that Eq. 17 reasonably correlates air/water froth height data.

8. The consequences of entrainment on tray efficiency, assuming that the tray above receives a uniform flux of entrainment throughout its cross-sectional area, is given by

$$\frac{E_{MV}(E)}{E_{MV}(E=0)} = 1-0.8E_{OG}\lambda_0^{0.543}E\frac{V_0}{L_0}. \tag{49}$$

Notation

C_{SB} = Souders–Brown flooding capacity factor, m/s
E_{MV} = apparent Murphree tray efficiency
$f(\phi_{2\phi})$ = see Eq. 34
F_{LV} = flow parameter for determining flood point
Fr = Froude number
g = acceleration due to gravity, 9.8 m/s^2
G = vapor mass-flow rate, kg/s
$h_{2\phi,ND}$ = no-drag solution for froth height, m
$h_{2\phi,WD}$ = solution for froth height that includes drag effects, m
h_W = exit weir height, m
L = liquid mass-flow rate, kg/s
T_S = tray spacing, m
v_F = vapor velocity under flooding conditions, m/s
V = dimensionless droplet velocity $= v_D/v_{D0}$

Greek letters

β = see Eq. 35
ϕ_e = effective froth density
$\phi_{2\phi}$ = average froth density $= h_L/h_{2\phi}$
ρ_L = liquid density, kg/m^3
ρ_V = vapor density, kg/m^3
ξ = dimensionless height $= z/h_{Fe}$

Literature Cited

Bain, J. L., and M. Van Winkle, "A Study of Entrainment, Perforated Plate Column—Air-Water System," *AIChE J.*, **7**, 363 (1961).

Bennett, D. L., R. Agrawal, and P. J. Cook, "New Pressure Drop Correlation for Sieve Tray Distillation Columns," *AIChE J.*, **29**, 434 (1983).

Bennett, D. L., and H. J. Grimm, "Eddy Diffusivity for Distillation Sieve Trays," *AIChE J.*, **37**, 589 (1991).

Colwell, C. J., "Clear Liquid Height and Froth Density on Sieve Trays," *Ind. Eng. Chem. Process Des. Dev.*, **20**, 298 (1981).

Fair, J. R., "How to Predict Sieve Tray Entrainment and Flooding," *Petro/Chem. Eng.*, **33**, 211 (1961).

Fair, J. R., D. E. Steinmeyer, W. R. Penney, and B. B. Crocker, "Liquid-Gas Systems," in *Perry's Chemical Engineers' Handbook*, 6th ed., D. W. Green and J. O. Maloney, eds., McGraw-Hill, New York, pp. 18–49 (1984).

Friend, L., E. J. Lemieux, and W. C. Schreiner, "New Data on Entrainment from Perforated Trays at Close Spacings," *Chem. Eng.*, **67**, 101 (1960).

Hofhuis, P. A. M., and F. G. Zuiderweg, "Sieve Plates: Dispersion Density and Flow Regimes," *Ind. Chem. Eng. Symp. Ser.*, **56**, 2.2/1 (1979).

Hughes, R. R., and E. R. Gilliland, "The Mechanics of Drops," *Chem. Eng. Prog.*, **48**, 497 (1952).

Hunt, C. d'A., D. N. Hanson, and C. R. Wilke, "Capacity Factors in the Performance of Perforated-Plate Columns," *AIChE J.*, **1**, 441 (1955).

Kister, H. Z., W. V. Pinczewski, and C. J. D. Fell, "Entrainment from Sieve Trays Operating in the Spray Regime," *Ind. Eng. Chem. Process Des. Dev.*, **20**, 528 (1981).
Kister, H. Z, and J. R. Haas, "Entrainment from Sieve Trays in the Froth Regime," *Ind. Eng. Chem. Res.*, **27**, 2331 (1988).
Lemieux, E. H., and L. H. Scotti, "Perforated Tray Performance," *Chem. Eng. Prog.*, **65**, 52 (1969).
Lockett, M. J., "The Froth to Spray Transition on Sieve Trays," *Trans. Inst. Chem. Eng.*, **59**, 26 (1981).
Lockett, M. J., *Distillation Tray Fundamentals*, Cambridge Univ. Press, New York (1986).
Lockett, M. J., G. T. Spiller, and K. E. Porter, "The Effect of the Operating Regime on Entrainment from Sieve Plates," *Trans. Inst. Chem. Eng.*, **54**, 202 (1976).
Lockett, M. J., M. A. Rahman, and H. A. Dhulesia, "The Effect of Entrainment on Distillation Tray Efficiency," *Chem. Eng. Sci.*, **38**, 661 (1983).
Nutter, D. E., "Weeping and Entrainment Studies for Sieve and V-Grid Trays in an Air-Oil System," *Ind. Chem. Eng. Symp. Ser.*, **56**, 3.2/47 (1979).
Pinczewski, W. V., N. D. Benke, and C. J. D. Fell, "Phase Inversion on Sieve Trays," *AIChE J.*, **21**, 1210 (1975).
Pinczewski, W. V., and C. J. D. Fell, "Froth to Spray Transition on Sieve Trays," *Ind. Eng. Chem. Process Des. Dev.*, **21**, 774 (1982).
Porter, K. E., and J. D. Jenkins, *Distillation 1979*, Inst. Chem. Eng., London (1979).
Puppich, P., and R. Goedecke, "Investigation of Entrainment in Tray Columns," *Chem. Eng. Technol.*, **10**, 224 (1987).
Repasky, J. M., D. L. Bennett, and J. C. Chen, "Sieve Tray Entrainment: Fraction of Liquid Flux which Passes to the Stage Above," AIChE Meeting, New Orleans (1992).
Sakata, M., and Y. Yanagi, "Performance of a Commercial Scale Sieve Tray," *Ind. Chem. Eng. Symp. Ser.*, **56**, 3.2/21 (1979).
Souders, M., and G. G. Brown, "Design of Fractionating Columns: I. Entrainment and Capacity," *Ind. Eng. Chem.*, **26**, 98 (1934).
Stichlmair, J., *Grundlagen der Dimensionierung des Gas/Flussigkeit Kontaktapparates Bodenkolonne*, Verlag Chemie, Berlin (1978).
Thomas, W. H., and O. Ogboja, "Hydraulic Studies in Sieve Tray Columns," *Ind. Eng. Chem. Process Des. Dev.*, **17**, 429 (1978).
Zuiderweg, F. J., "Sieve Trays: A View on the State of the Art," *Chem. Eng. Sci.*, **37**, 1441 (1982).

Manuscript received Aug. 2, 1991, and revision received Nov. 1, 1994.